Ultra Stable Microwave Radiometers for Future Sea Surface Salinity Missions

William J. Wilson, Alan Tanner
Jet Propulsion Laboratory, California Institute of Technology
Pasadena, CA 91109

Fernando Pellerano
Goddard Space Flight Center
Greenbelt, MD 20771

Abstract- Future Sea Surface Salinity missions will require measurements with an accuracy of 0.1 psu. This will require the L-band radiometers to have calibration stabilities of $\leq$ 0.05 K over 2 days. This research will determine the optimum radiometer requirements and configuration to achieve $\leq$ 0.05 K calibration stability. This will be followed by building and testing breadboard radiometers to demonstrate the optimum radiometer.

I. Introduction

Measurements of sea surface salinity (SSS) are important in understanding the response of the ocean to the global water cycle and climate changes. The SSS variability is the key tracer for freshwater input and output to the ocean associated with precipitation, evaporation, ice melting, and river runoff. Accurate measurements of SSS, along with sea surface temperature, will determine the sea surface density, which controls the formation of water masses and regulates the 3-dimensional ocean circulation.

The proposed Earth Science System Pathfinder (ESSP) mission Aquarius, will measure global SSS with 100 km spatial resolution every 8-days with an average monthly SSS accuracy of 0.2 psu (parts per thousand) over the oceanic salinity range of 32 to 38 psu. The calibration stability requirement for the Aquarius radiometers is 0.15 K over two days. Future SSS missions will require SSS measurements with an accuracy of 0.1 psu and with a smaller spatial resolution. This will require the L-band radiometers to have calibration stabilities of $\leq$ 0.05 K over 2 days. Note that this is a factor of 3 improvement over the Aquarius radiometer requirement.

The main focus of this Instrument Incubator Program (IIP) research is to analytically determine the optimum radiometer requirements and configuration to achieve the $\leq$ 0.05 K calibration stability. This will be followed by building and testing breadboard radiometers to demonstrate this optimum radiometer configuration in preparation for future salinity missions.

II. Radiometer Model

At the lower microwave frequencies, with large antenna feedhorns, it is not possible to calibrate with external thermal loads through the feedhorn because the loads would be too large. Therefore, the radiometer calibration must be done following the feedhorn. One practical way to do this is to couple a stable noise diode source into the radiometer and to periodically switch to a reference load (Dicke switch) for radiometer noise, gain and offset calibration. This calibration must be done frequently to insure that the radiometer noise, gain and offset changes do not add noise to the calibration. (In this calibration method, the emission and loss of the feedhorn and orthomode transducer (OMT) must be modeled and the measurements corrected.)

It is an interesting problem to determine the noise diode calibration and reference switching sequence and the system requirements to optimize the radiometer sensitivity and calibration stability. Our initial study has focused on the 3 positions Dicke switching sequence as described below. This technique was used in two of our recent radiometer systems, the Advanced Water Vapor Radiometer (AWVR) [1] and the Passive/Active L and S-band (PALS) system [2].

A model of a typical radiometer is shown in Fig. 1. In this radiometer configuration, the noise diode calibration source is coupled into the radiometer as close to the feedhorn as possible. (This is a simplified example, since in the actual radiometer, multiple noise diodes will be coupled at various points for improved accuracy and stability.)

A diagram of the 3-position switching sequence is shown in Fig. 2. In this sequence, a third of the time is spent looking through the antenna ($\mathbf{V_a}$), a third through the antenna plus noise diode ($\mathbf{V_n}$), and a third switched to the reference load ($\mathbf{V_o}$).

When the radiometer is switched to the antenna input, the output voltage is:

$$\mathbf{V_a} = \mathbf{G}*\left(\frac{\mathbf{T_a}}{\mathbf{L}} + \mathbf{T_L}*\left(\mathbf{1} - \frac{\mathbf{1}}{\mathbf{L}}\right) + \mathbf{T_r}\right) + \mathbf{Z}, \qquad (1)$$

where $\mathbf{T_a}$ = antenna temperature
$\mathbf{T_L}$ = input loss temperature
$\mathbf{L}$ = input loss
$\mathbf{T_r}$ = radiometer noise temperature

G = Gain of radiometer
Z = Zero offset of output circuits.

When the noise diode is turned on, the radiometer output voltage is:

$$\mathbf{V_n = G*(\frac{T_a}{L} + T_L*\left(1 - \frac{1}{L}\right) + T_r + T_n) + Z}, \qquad (2)$$

where $\mathbf{T_n}$ = noise diode temperature.

When the radiometer is switched to the reference load, the radiometer output voltage is:

$$\mathbf{V_o = G*(T_o + T_r) + Z}, \qquad (3)$$

where $\mathbf{T_o}$ = reference load temperature.

One of the most stable data processing methods to calculate the antenna temperature uses these three measurements with the following expression:

$$\mathbf{T_a = T_L + L*\left[T_o - T_L - \frac{(V_o - V_a)}{(V_n - V_a)}*T_n\right]}. \qquad (4)$$

The advantage of this technique is that all the variable radiometer parameters ($\mathbf{T_r}$, **G**, and **Z**) are either subtracted or divided out at the fast switching rate. (The switching rate must be faster that the $1/f_{knee}$ of the $\mathbf{T_r}$, **G,** and **Z** noise spectra.)

One practical problem with this technique is that the temperatures in this equation, $\mathbf{T_L}$, $\mathbf{T_o}$ and $\mathbf{T_n}$, must be known to a high precision. (A reasonable assumption is that the input loss, **L**, will be known and will be stable.) A sensitivity analysis has been done on this equation with the following results.

The change in antenna temperature with respect to the reference temperature, $\mathbf{T_o}$, is given by:

$$\mathbf{\partial T_a = L*\partial T_o}. \qquad (5)$$

With a front-end loss of ~ 1 dB (1.25), it will be necessary to measure $\mathbf{T_o}$ to an accuracy of 0.02 C, to keep $\delta\mathbf{T_a}$ < 0.025 K. This will be possible since the reference load is a small device and a temperature sensor can accurately measure its temperature.

The change in the antenna temperature with respect to the input loss temperature, $\mathbf{T_L}$, is given by:

$$\mathbf{\partial T_a = (1 - L)*\partial T_L}. \qquad (6)$$

With a front-end loss of ~1 dB, it will be necessary to control the temperature of the radiometer front-end components, $\mathbf{T_L}$, to ±0.1° C, to achieve a change in $\delta\mathbf{T_a}$ < 0.025 K. (It is not sufficient to measure the temperatures of the front-end components, since the time constant of the component temperatures where the loss occurs is not known well enough to accurately predict their temperature.)

The change in the antenna temperature with respect to the noise diode temperature, $\mathbf{T_n}$, is given by:

$$\mathbf{\partial T_a = L*\frac{(V_o - V_a)}{(V_n - V_a)}*\partial T_n}. \qquad (7)$$

With a front-end loss of ~1 dB, the noise diode temperature must be stable to ~$2x10^{-4}$ to achieve the $\mathbf{T_a}$ stability < 0.025 K. With careful temperature control, and using a constant current source to power the noise diode, noise diode stabilities of $3x10^{-5}$ have been achieved in the AWVR [1]. Thus, with careful control, this requirement can be met.

Taking the root mean square of these three terms, gives the result that $\mathbf{T_a}$ will meet the stability requirement of ≤ 0.05 K.

To calculate the RMS noise of this measurement, it is useful to consider each of the voltage measurements to be equal to its expected value plus a noise term. The noise is a small fraction of the expected value and can be modeled as an additive Gaussian random variable with zero mean. Thus each voltage can be modeled with the following expression: $\mathbf{V_i = \langle V_i \rangle *(1 + \delta_i)}$, where i represents the three measurements described above. The measurement time for each interval is $\tau/\mathbf{3}$ seconds and the bandwidth is **B** Hz, so that the expectation of the random variable $\langle \delta_i \rangle^2 = \frac{\mathbf{3}}{\mathbf{B}\tau}$.

Substituting the noise approximations into the expression for $\mathbf{T_1}$ in (4), the RMS value or NEDT (Noise Equivalent Delta Temperature) of the measurement of $\mathbf{T_a}$ can be derived. Since the random variables, δ_i, are independent and zero mean, the NEDT for the antenna temperature $\mathbf{T_a}$ is given by:

$$\mathbf{\Delta T_a = L*\sqrt{\frac{3}{B\tau}}*\sqrt{(T_o + T_r)^2 + (T_1 + T_r)^2*\left[1 - \frac{(T_o - T_1)}{T_n}\right]^2 + (T_1 + T_r + T_n)^2*\left[\frac{T_o - T_1}{T_n}\right]^2}} \qquad (8)$$

where $\mathbf{T_1 = \frac{T_a}{L} + T_L*\left(1 - \frac{1}{L}\right)}$.

The value of D$\mathbf{T_a}$ is plotted as a function of $\mathbf{T_a}$ in Fig. 3, for a set of parameters that is representative for ocean measurements with the Aquarius radiometer: $\mathbf{T_o}$ = 290 K, $\mathbf{T_r}$ = 180 K, $\mathbf{T_n}$ = 300 K, **B** = 25 MHz and t = 12 sec. The minimum NEDT is 0.07 K for these conditions.

The advantage of this technique is that it improves the calibration stability by removing variations in $\mathbf{T_r}$, **G** and **Z**. The disadvantage is that the NEDT is ~15% larger than with the standard Dicke switched radiometer and a factor of 2.7 larger than for a total power radiometer assuming perfect calibration. (The NEDT is greater because more time is spent on calibrating the gain, radiometer noise and offset.) One of the tasks we are working on is to determine the best operating sequence to meet the tight stability requirements and also achieve the lowest NEDT, since the goal for future SSS missions is to reduce the NEDT to a minimum.

III. Experimental Results

During the summer of 2001, improvements to the PALS temperature control of the front-end components (including the OMT, the noise diode and coupler and the Dicke switch) in the L-band radiometer were made. The thermal controller had ±0.1° C temperature stability. Following these modifications, a series of sky measurements were made. For these sky measurements, the radiometer and horn were pointed horizontally and a 45° angle plate was used to reflect the antenna beam to the zenith direction as shown in Fig. 4. The sky measurements from three days of data are shown in Fig. 5. These data show that with the excellent temperature control, this radiometer system achieved ~ 0.05 K calibration stability over a 3-day period. These results give confidence that this approach is on the correct path.

IV. Summary

What has been learned from the AWVR and PALS measurements is that with careful temperature control of the critical radiometer components, it is possible to achieve excellent calibration stabilities. However, the 3-position Dicke switching sequence increases the NEDT to larger than desired levels. Analytical expressions are being developed to optimize the observing switch sequence, which will be based on the measured noise spectra of the radiometer parameters. Another area of our research is to analyze the effect of VSWR on the calibration components. The results of this analysis will be tested in the laboratory on the breadboard radiometers to demonstrate this theory.

Another aspect of this research is to reduce the size of the L-band radiometers. This will enable the tight temperature control in space that is required. A radiometer using small microwave integrated components is being built and will be tested.

Acknowledgment

This work represents one phase of research carried out at the Jet Propulsion Laboratory, California Institute of Technology, under contract with the National Aeronautic Space Administration.

References

[1] Tanner, A. B., A high stability Ka-band radiometer for tropospheric water vapor measurements," Aerospace and Electronic Systems Symposium Proceedings, Big Sky Montana, March 2001.

[2] W. J. Wilson, S. H. Yueh, S. J. Dinardo, S. Chazanoff, A. Kitiyakara, F. K. Li, and Y. Rahmat-Samii, "Passive active L- and S-band (PALS) microwave sensor for ocean salinity and soil moisture measurements," *IEEE Trans. Geosci. Remote Sensing*, vol. 39, pp. 1039-1048, May 2001.

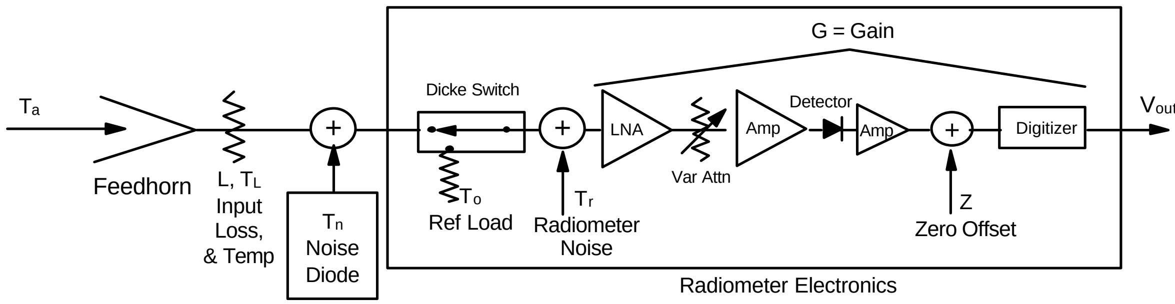

Figure 1. Simplified Radiometer Block Diagram

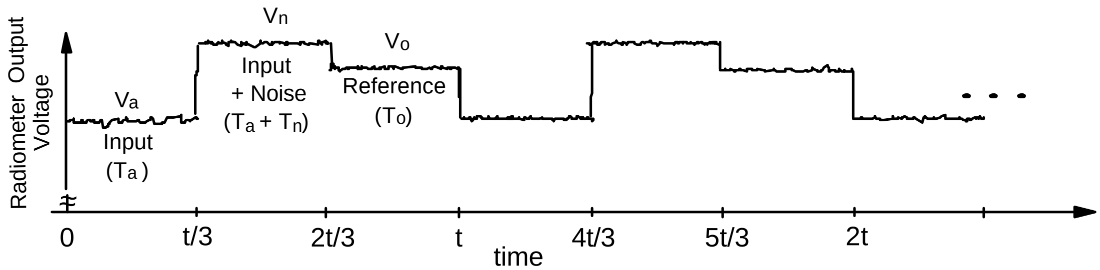

Fig. 2. Radiometer 3 position switching sequence

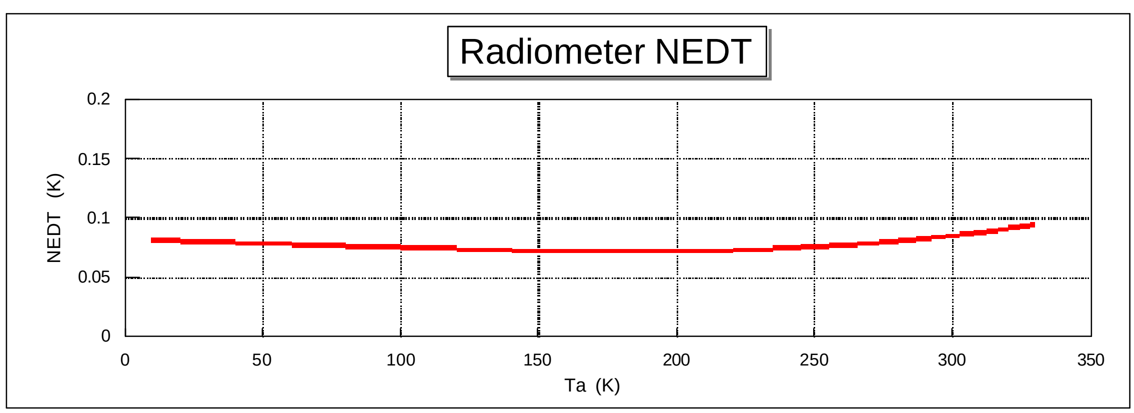

Fig. 3. Radiometer NEDT using 3-position switching sequence from equation (8). A set of parameters that is representative for ocean measurements with the Aquarius radiometer: $\mathbf{T_o}$ = 290 K, $\mathbf{T_r}$ = 180 K, $\mathbf{T_n}$ = 300 K, $\mathbf{B}$ = 25 MHz and t = 12 sec, was used for this plot.

Figure 4. PALS instrument in sky measurement configuration, showing the horizontal radiometer and horn, and the 45° angle reflector directing the bean to the zenith.

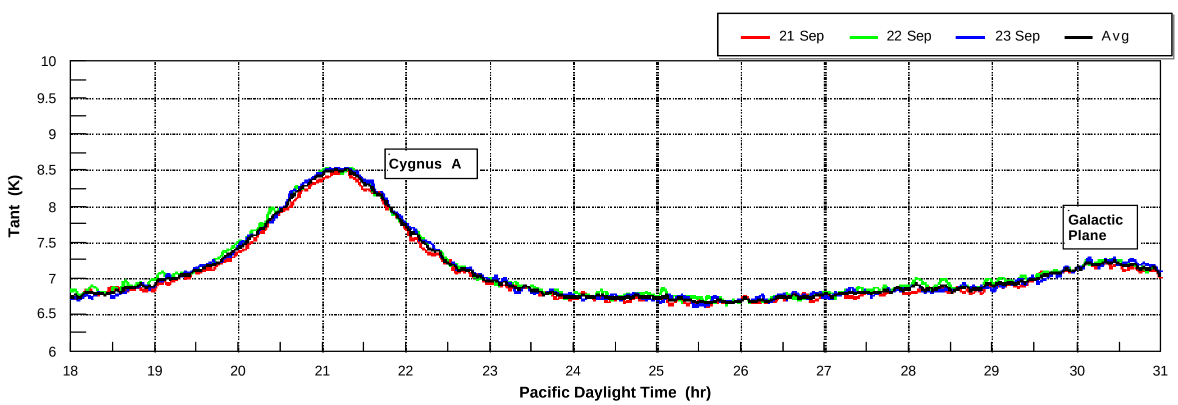

Figure 5. A 0.05 K calibration stability was demonstrated by the zenith sky data taken during the PALS L-band radiometer sky calibration experiment on 21, 22, and 23 September 2001. The strong signals from Cygnus A and the galactic plane agree with the L-band sky survey.